

Probing the Innermost Part of AGN Tori with the Near-Infrared CO Absorption Band

SHUNSUKE BABA,^{1,2} TAKAO NAKAGAWA,¹ NAOKI ISOBE,¹ AND MAI SHIRAHATA¹

¹*Institute of Space and Astronautical Science, Japan Aerospace Exploration Agency, 3-1-1 Yoshinodai, Chuo-ku, Sagami-hara, Kanagawa 252-5210, Japan*

²*Department of Physics, Graduate School of Science, The University of Tokyo, 7-3-1 Hongo, Bunkyo-ku, Tokyo 113-0033, Japan*

ABSTRACT

We analyzed the 4.67 μm CO ro-vibrational absorption band in nearby ten active galactic nuclei (AGNs) observed with *AKARI* and *Spitzer* by fitting a plane-parallel local thermal equilibrium gas model. We found that the CO gas is warm (200–500 K) with a large column density ($N_{\text{H}} \gtrsim 10^{23} \text{ cm}^{-2}$). Such a large column of warm gas is not achievable with UV heating or shock heating in starbursts. The most convincing heating source is X-ray photons emitted from the nuclei, which can produce warm gas of $N_{\text{H}} \sim 10^{24} \text{ cm}^{-2}$. This indicates that the region probed by the CO absorption is in the vicinity of the nuclei. The hydrogen column density estimated from the CO band is smaller than that inferred from X-ray observations. The observed deep absorption implies that the gas is close to the continuum source. We suggest that the probed region is outside the X-ray emitting region and just in front of the dust sublimation layer, which can be designated as the inner rim of the obscuring material around the AGNs.

Keywords: galaxies: active — galaxies: nuclei — infrared: galaxies

1. INTRODUCTION

The dichotomy of active galactic nuclei (AGNs) in the presence or absence of broad optical emission lines has been attributed a geometrical effect caused by a putative AGN torus, an optically and geometrically thick torus-shaped dusty cloud (Antonucci 1993). However, it is difficult to directly image AGN tori because of their small sizes on parsec scales, even with recent millimeter to sub-millimeter interferometric observations.

The spectroscopy of a near-infrared absorption can potentially achieve a high-spatial resolution toward an AGN because the near-infrared continuum would be dominated by the compact central region. Shirahata et al. (2013) observed the CO fundamental ro-vibrational band centered at 4.67 μm ($\nu = 1 \leftarrow 0$, $\Delta J = \pm 1$) toward the obscured AGN IRAS 08572+3915 with the Subaru telescope and found that the CO gas is warm and has a large column density. This suggests that the observed CO gas should be close to the nucleus being heated by the X-ray radiation, which has a high penetrating power. The CO feature, however, does not always appear in all type-2 AGNs, where the torus is assumed to be edge-on. Lutz et al. (2004) observed nearby 12 type-2 galaxies with *ISO*, but none of them show the CO absorption. This fact questions the hypothesis that the CO absorption probes warm gas near the central region. The origin of the CO absorption should be ascertained.

In the *AKARI* mission program AGNUL during the cryogenic phase, six galaxies exhibit the CO absorption: IRAS 06035–7102, 08572+3915, 19254–7245, 23128–5919, UGC 5101, and Mrk 273. From the *Spitzer*/IRS observations, Spoon et al. (2005) reported that four galaxies show the feature: IRAS 00182–7112, 00397–1312, 00406–3127, and 13352+6402. All of these ten galaxies possess AGN signatures in infrared and/or X-ray properties. In this study, we analyzed the ten AGNs to investigate where the CO absorption originates.

2. OBSERVATIONS AND DATA REDUCTION

We followed Baba et al. (2016) in the data reduction of the *AKARI* near-infrared grism mode observations to correct for the effect of the second-order light contamination. To minimize the uncertainty in the wavelength calibration, the wavelength origin was adjusted from the value reported by the toolkit by a few pixels based on the positions of some emission features.

Because we were not able to determine the continuum level at longer wavelengths than the CO absorption from the *AKARI* observations themselves, we complimented them with the calibrated *Spitzer*/IRS spectra downloaded from the

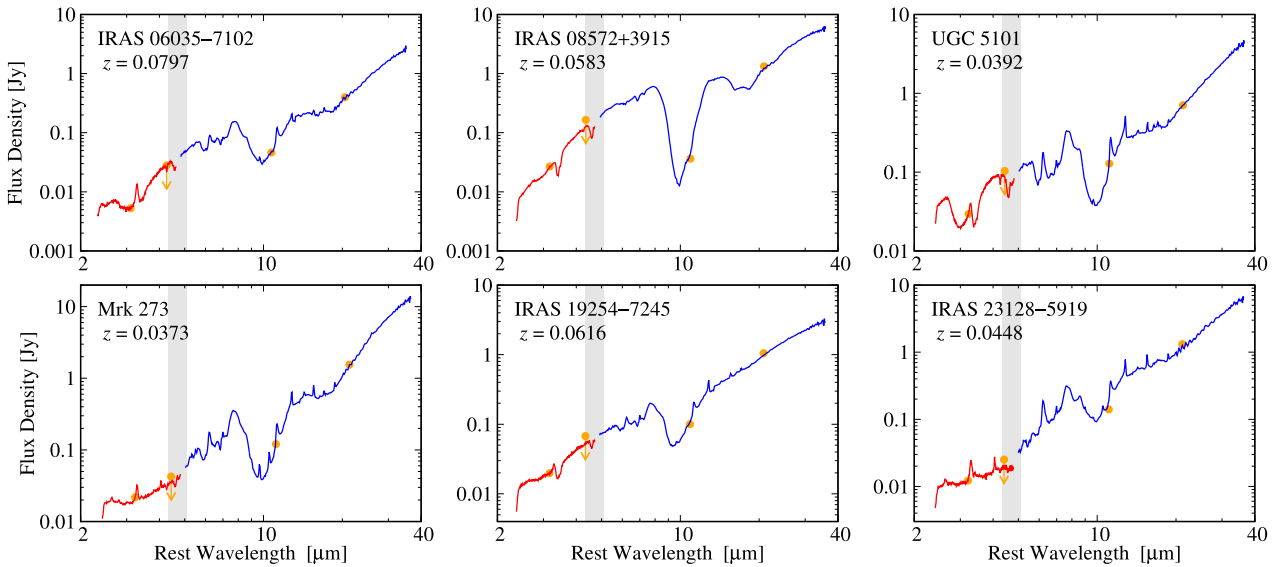


Figure 1. Combined spectrum of each *AKARI* target. Red and blue curves show the *AKARI*/IRC and *Spitzer*/IRS spectra, respectively. Orange filled circles represent the *WISE* photometric fluxes. The *AKARI* and *Spitzer* spectra are scaled so that they match the *WISE* points, but the *W2* band ($4.6 \mu\text{m}$ in the observed frame) flux shown with a downward arrow was used only as an upper limit. The wavelength range of the CO absorption is indicated by a gray rectangle.

Spitzer Heritage Archive. We scaled the IRC and IRS spectra along the flux axis so that they match the *WISE* magnitudes to reduce the effect of the different aperture sizes between the two instruments. The resultant combined spectra are shown in Figure 1.

The IRS spectra of the targets selected from the sample of [Spoon et al. \(2005\)](#) were also taken from the *Spitzer* Heritage Archive. These spectra entirely cover the CO absorption within themselves. We did not apply any scaling to them because only the continuum-normalized spectra were used in the analysis. In IRAS 00397 and 13352, because the observed CO profile appeared to be systematically displaced to shorter wavelengths from the predicted position, we manually shifted the data points by 0.009 and $0.010 \mu\text{m}$, respectively.

3. ANALYSIS

We used the plane-parallel local thermal equilibrium (LTE) gas model developed by [Cami \(2002\)](#) to analyze the absorption profile assuming that the CO gas comprises a single component with uniform number density, temperature, and turbulent velocity (velocity width). Any isotopomers other than $^{12}\text{C}^{16}\text{O}$ were included. The continuum was set to a blackbody with a sublimation temperature of 1500 K ([Barvainis 1987](#)) based on the assumption that the background source is an optically thick hot dust sublimation layer. The model gives the ratio of the absorbed flux to the background. We normalized each spectrum around the CO absorption with a continuum level estimated as a cubic spline curve interpolated between pivots at 4.15 , 4.35 , 5.10 , and $5.40 \mu\text{m}$, and then fitted the model to the data via three free parameters: the CO column density N_{CO} , temperature T_{CO} , and turbulent velocity v_{turb} . The fitting wavelength range was $4.35\text{--}5.10 \mu\text{m}$.

4. RESULTS

Figure 2 shows the normalized spectra and the best-fitted CO gas models. The observed absorption is deep, which requires close-to-unity area covering factors. This indicates the CO gas exists near the continuum source. The reduced χ^2 values ($\chi_v^2 \equiv \chi^2/\text{dof}$) are quite high. We consider that these poor fits originate from the difficulty in determining the continuum level. We found that the CO gas has a high temperature and a large column density. The average T_{CO} is 360 K , which is far higher than the typical temperature of molecular gas in ordinary star-forming regions ($10\text{--}10^2 \text{ K}$, [Hollenbach & Tielens 1999](#)). The logarithm of N_{CO} in units of cm^{-2} is on average 19.5 , which corresponds to a molecular hydrogen column density of $\log N_{\text{H}_2} \sim 23.5$ if a CO abundance of $[\text{CO}]/[\text{H}_2] = 10^{-4}$ is adopted.

5. DISCUSSION

The observed CO gas has a high temperature and a large column density. We consider what mechanism can heat the observed large columns of warm gas.

The first candidate is ultraviolet (UV) photons. An intense UV radiation field incident on a cloud forms a photon-dominated region (PDR). [Meijerink & Spaans \(2005\)](#) modeled the PDR at four conditions. The maximum gas temperature is higher than 10^3 K in three cases. However, the temperature steeply drops to 10^2 K at column densities smaller than

NIR CO ABSORPTION IN AGN TORI

O36 - 3

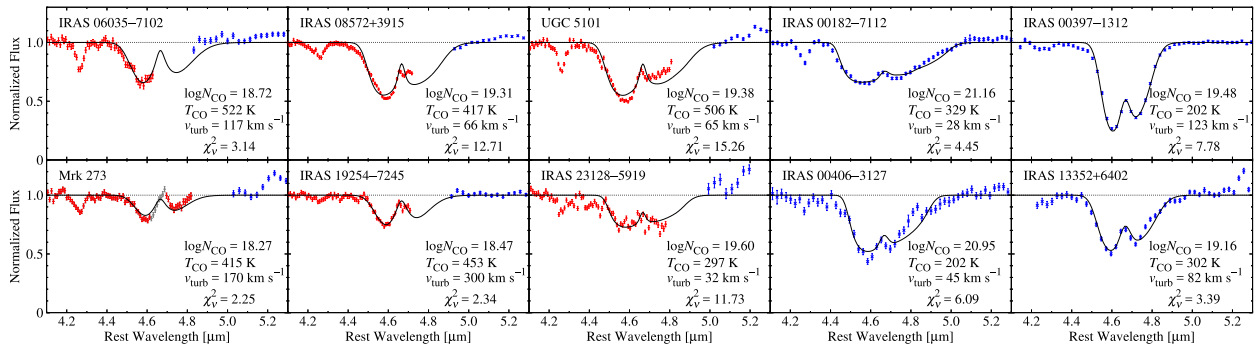


Figure 2. The result of the gas-model fitting for each target. A black solid line denotes the best-fit CO absorption profile. Red and blue points represent the data from the *AKARI*/IRC and *Spitzer*/IRS spectra, respectively. Gray points in Mrk 273, for which Yano et al. (in prep.) point the possibility of a peculiar ionized environment, were excluded from the fitting to avoid the possible contribution from the Pf β (4.65 μ m) emission. The best-fit parameters and the goodness-of-fit $\chi^2_v \equiv \chi^2/\text{dof}$ are noted at the right bottom corner.

$N_{\text{H}} = 10^{22} \text{ cm}^{-2}$ because of the strong attenuation by dust. The achievable warm ($>10^2 \text{ K}$) CO column density is only $N_{\text{CO}} \sim 10^{16} \text{ cm}^{-2}$, far smaller than the observed values.

The next candidate is shock heating. A number of studies have discussed the physical and chemical processes in shocks (e.g., Hollenbach & McKee 1989; Neufeld & Dalgarno 1989). With a shock velocity of $\sim 100 \text{ km s}^{-1}$ and a pre-shock density of $10^4\text{--}10^6 \text{ cm}^{-3}$, the initial post-shock temperature exceeds 10^4 K . Under the balance between the OH cooling and heating due to the H_2 formation on dust grains, the temperature remains at $\sim 10^2 \text{ K}$. The scale of this warm gas layer is $N_{\text{H}} \lesssim 10^{22} \text{ cm}^{-2}$ or $N_{\text{CO}} \lesssim 10^{18} \text{ cm}^{-2}$. This upper bound is comparable to the smallest values we observed. While there is still room for a partial contribution from shock heating, UV heating cannot fully account for the heating mechanism of the CO gas.

The third candidate is X-ray photons emitted from the nuclear region of an AGN. A strong X-ray radiation field incident on a cloud creates an X-ray-dominated region (XDR). X-ray photons can penetrate more deeply into clouds than UV due to their small cross sections. Meijerink & Spaans (2005) modeled XDRs with chemical reactions under four conditions (density $n_{\text{H}} = 10^3$ or $10^{5.5} \text{ cm}^{-3}$, and X-ray flux $F_{\text{X}} = 1.6$ or $160 \text{ erg cm}^{-2} \text{ s}^{-1}$). In all cases except for that of the high density and low flux, the simulated temperatures are in the range $10^2\text{--}10^4 \text{ K}$. Moreover, the temperatures remain higher than 10^2 K up to column densities of $N_{\text{H}} \sim 10^{24} \text{ cm}^{-2}$. This scale of heating is more than two orders of magnitude larger than those of the previous two mechanisms. In all the cases, N_{CO} reaches 10^{18} cm^{-2} before the temperature falls to 10^2 K , indicating that XDRs can account for the observed warm CO gas of a large column density. We suggest that the most reasonable heating mechanism of the observed warm CO gas is X-ray heating, which leads to the further conclusion that the observed gas is in the vicinity of the nucleus. Although the possibility that shock heating accounts for a substantial fraction of the total power cannot be ruled out in some objects, its contribution must be smaller than that of X-ray photons.

To clarify the location of the region in which the CO absorption originates, we compared the CO column density with the hydrogen column density estimated through an X-ray spectral analysis (Brightman & Nandra 2011). Four objects in their sample are common with our targets: UGC 5101, Mrk 273, IRAS 19254, and IRAS 23128. We converted N_{CO} into N_{H} assuming an abundance ratio yielded in the high-density XDR models of Meijerink & Spaans (2005) ($N_{\text{CO}}/N_{\text{H}} \sim 10^{-4}$). Figure 3(a) compares the two hydrogen column densities. The hydrogen column density derived from the CO absorption, $N_{\text{H},4.67}$, is 2–30 times smaller than that inferred from the X-ray spectral analysis, $N_{\text{H},\text{X}}$. This comparison indicates that the two columns trace the amount of gas at different depths. The X-ray-derived column density $N_{\text{H},\text{X}}$ measures the gas in front of the central AGN nucleus using the X-ray radiation from it as the background. By contrast, $N_{\text{H},4.67}$ should measure the gas outside the X-ray emitting region, tracing a smaller amount of the foreground gas. This consideration is consistent with the assumption that the near-infrared background continuum source is the region heated by the nucleus. We suggest that the CO absorption originates in the molecular gas distributed outside the X-ray emitting region.

Another indicator of the degree of obscuration is the optical depth of the 9.7 μ m silicate dust absorption $\tau_{9.7}$. We converted $\tau_{9.7}$ measured by Dartois & Muñoz-Caro (2007); Imanishi et al. (2007); Imanishi (2009) into N_{H} using two relations $A_{\text{V}}/\tau_{9.7} = 18.0 \text{ mag}$ (Whittet 2003) and $N_{\text{H}}/A_{\text{V}} = 1.9 \times 10^{21} \text{ cm}^{-2} \text{ mag}^{-1}$ (Bohlin et al. 1978). Figure 3(b) compares the resultant hydrogen column density $N_{\text{H},9.7}$ with $N_{\text{H},4.67}$. In contrast to the comparison with X-ray observations, $N_{\text{H},4.67}$ is similar to or a bit larger than $N_{\text{H},9.7}$. We suggest that the observed CO gas and silicate dust roughly coexist in the same region.

6. SUMMARY

We have presented the result of the analysis of the CO ro-vibrational absorption band (4.67 μ m) toward nearby ten AGNs observed with *AKARI* and *Spitzer*. The CO column density and gas temperature were estimated for each target with the use of a plane-parallel LTE gas model. The average CO column density was found to be $N_{\text{CO}} \sim 10^{19.5} \text{ cm}^{-2}$, which

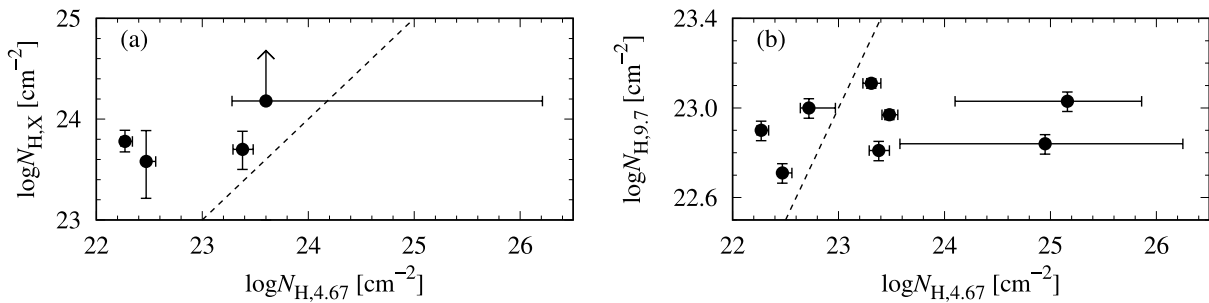


Figure 3. The hydrogen column density estimated from the CO absorption is compared with those derived from (a) an X-ray analysis and (b) the 9.7 μm silicate dust absorption strength. The dashed lines denote the identity.

corresponds to a hydrogen column density of $N_{\text{H}} \sim 10^{23.5} \text{ cm}^{-2}$. This large column density indicates that the AGNs are heavily obscured. The average temperature was found to be 360 K, which is much higher than the typical value in normal star-forming regions.

The observed large columns of the warm gas cannot be reproduced by UV heating or shock heating. We suggest that the most convincing heating source is X-ray photons emitted from the central engines, which in addition suggests that the region probed by the CO absorption should be in the vicinity of the nuclei.

A comparison with an X-ray spectral analysis shows that the hydrogen column density derived from the CO absorption is 2–30 times smaller than that inferred from the X-ray analysis. We suggest that the region probed by the near-infrared CO absorption is located outside the X-ray emitting region. The close-to-unity covering factor of the CO gas indicates that the gas is close to the continuum source, which we hypothesize to be the dust sublimation layer at the inner rim of the obscuring material around the AGN. In contrast to the comparison with the X-ray observations, the hydrogen column density derived from CO absorption is similar to or a bit larger than that calculated from the optical depth of the 9.7 μm silicate dust absorption. We suggest that CO-absorbing gas and silicate dust roughly coexist in the same region.

ACKNOWLEDGMENTS

This work is supported by Grant-in-Aid for JSPS Research Fellows Grant Number JP17J01789 (S.B.) and for Scientific Research Grant Number JP26247030 (T.N.). This research is based on observations with *AKARI*, a JAXA project with the participation of ESA. This work is based on observations made with the *Spitzer Space Telescope*, obtained from the NASA/IPAC Infrared Science Archive, both of which are operated by the Jet Propulsion Laboratory, California Institute of Technology under a contract with the National Aeronautics and Space Administration. This publication makes use of data products from the Wide-field Infrared Survey Explorer, which is a joint project of the University of California, Los Angeles, and the Jet Propulsion Laboratory/California Institute of Technology, and NEOWISE, which is a project of the Jet Propulsion Laboratory/California Institute of Technology. *WISE* and NEOWISE are funded by the National Aeronautics and Space Administration.

REFERENCES

- Antonucci, R. 1993, *ARA&A*, 31, 473
 Baba, S., Nakagawa, T., Shirahata, M., et al. 2016, *PASJ*, 68, 27
 Barvainis, R. 1987, *ApJ*, 320, 537
 Bohlin, R. C., Savage, B. D., & Drake, J. F. 1978, *ApJ*, 224, 132
 Brightman, M., & Nandra, K. 2011, *MNRAS*, 413, 1206
 Cami, J. 2002, PhD thesis, University of Amsterdam
 Dartois, E., & Muñoz-Caro, G. M. 2007, *A&A*, 476, 1235
 Hollenbach, D., & McKee, C. F. 1989, *ApJ*, 342, 306
 Hollenbach, D. J., & Tielens, A. G. G. M. 1999, *Reviews of Modern Physics*, 71, 173
 Imanishi, M. 2009, *ApJ*, 694, 751
 Imanishi, M., Dudley, C. C., Maiolino, R., et al. 2007, *ApJS*, 171, 72
 Lutz, D., Sturm, E., Genzel, R., Spoon, H. W. W., & Stacey, G. J. 2004, *A&A*, 426, L5
 Meijerink, R., & Spaans, M. 2005, *A&A*, 436, 397
 Neufeld, D. A., & Dalgarno, A. 1989, *ApJ*, 340, 869
 Shirahata, M., Nakagawa, T., Usuda, T., et al. 2013, *PASJ*, 65, 5
 Spoon, H. W. W., Keane, J. V., Cami, J., et al. 2005, *Astrochemistry: Recent Successes and Current Challenges*, 231, 281
 Whittet, D. C. B., ed. 2003, *Dust in the galactic environment*, 2003 Series in Astronomy and Astrophysics, ISBN 0750306246